International Conference on Mathematics, Computational Methods & Reactor Physics (M&C 2009)
Saratoga Springs, New York, May 3-7, 2009, on CD-ROM, American Nuclear Society, LaGrange Park, IL (2009)

PWR ASSEMBLY TRANSPORT CALCULATION: A VALIDATION BENCHMARK USING DRAGON, PENTRAN, AND MCNP

Tanguy Courau*
EDF R&D/SINETICS
1 av du Général de Gaulle
F92141 Clamart CEDEX, France
tanguy.courau@edf.fr

Glenn Sjoden
Nuclear and Radiological Engineering Department
University of Florida
202 Nuclear Science Building
Gainesville, FL32611, USA
sjoden@ufl.edu

Guy Marleau
Institut de Génie Nucléaire
École Polytechnique de Montréal
C.P. 6079, succ. Centre-ville
Montréal, Québec, Canada H3C 3A7
guy.marleau@polymtl.ca

ABSTRACT

This paper presents a 2D PWR fuel assembly benchmark performed with 3 transport codes: DRAGON which uses the collision probability method, PENTRAN, an S_n transport code, and MCNP, a Monte Carlo code.

First, DRAGON was used to produce a 2-group pin-by-pin cross-section library associated with 45 materials that describe the fuel assembly. Using the same library, it was then possible to perform comparisons between DRAGON and MCNP, and between PENTRAN and MCNP. Here, MCNP was considered as the reference multigroup Monte Carlo tool used to validate the deterministic codes. This type of 2-group benchmark can be utilized to evaluate the performance of different solvers using the very same cross-sections. The transport solutions provided here may be used as references for further comparisons with industrial reactor core codes using a diffusion or a SP_n solver, and generally relying on 2-group cross-sections.

Results show an excellent overall agreement between the 3 codes, with discrepancies that are less than 0.5% on the pin-by-pin flux, and less than 20 pcm on the k_{eff}. Therefore, it may be concluded that these deterministic codes are reliable tools to perform criticality transport calculations for PWR lattices.

Moreover, the use of multigroup Monte Carlo appears as an efficient independent technique to perform detailed code to code comparisons relying on the same cross-section library.

The present work may be considered as the first step of a 3D PWR core benchmark using DRAGON generated cross-sections and comparing PENTRAN and MCNP multigroup calculations.

Key Words: DRAGON, MCNP, PENTRAN, PWR

*Currently appointed as visiting research scientist at the University of Florida

1. INTRODUCTION

In an attempt to evaluate the potentialities of S_n methods applied to full core 3D parallel computations, EDF R&D is involved in a collaboration with the University of Florida. In this context, a 3D PWR core benchmark was proposed.

Prior to dealing with a full core calculation, it was decided to perform a detailed 2D benchmark modeling a PWR fuel assembly with 3 transport codes: DRAGON [1], which uses the collision probability method, PENTRAN [2, 3], an S_n transport code, and MCNP [4], a Monte Carlo code.

DRAGON was also used to produce a 2-group pin-by-pin cross-section library associated with the 45 materials describing the fuel assembly. After some minor cross-section reformatting, one generated a 2-group pin-specific library that could be used by all the codes selected for this benchmark.

It was then possible to perform comparisons, based on the same cross-section library, between DRAGON and MCNP, and between PENTRAN and MCNP, assuming MCNP to be the reference tool used to validate the deterministic codes.

After a convergence analysis, this paper compares the 2 deterministic transport solvers used here. These codes may provide reference deterministic transport solutions for further comparisons with various solvers, such as diffusion or SP_n, used at the core level for industrial calculations.

2. CROSS SECTION LIBRARY PRODUCED WITH DRAGON

The 2-group condensed cross-section library used is generated with DRAGON, after performing a 172-group transport calculation and homogenizing a 17x17 PWR assembly on a basis of individual fuel pins. The 172-group cross-section library used by DRAGON is based on the ENDF/B6 evaluation and was provided by the Wims Library Update Project [5].

Taking into account the $1/8^{th}$ symmetry of the assembly, the DRAGON heterogeneous geometry [6] presented in Figure 1 involves 1217 regions. The 1217-region, 172-group flux computed by DRAGON was then used for generation of a 2-group, 45-material cross-section library with an energy boundary set to the standard value of 0.625 eV. Moreover, an SPH transport – transport equivalence [7] was used within DRAGON to ensure reaction rate preservation before and after performing the flux weighted homogenization/condensation process. As a consequence, the DRAGON 2-group pin-by-pin reaction rate is identical to the homogenized and condensed 1217-region, 172-group reaction rate. Therefore, results presented here are limited to 2-group data.

Having stored the 45-material cross-section library in a DRAGON output file, 2 Python scripts [8] were written to translate these data into libraries compatible with PENTRAN and multigroup MCNP formats. This procedure therefore enables one to perform comparisons between DRAGON, MCNP, and PENTRAN based on a single multigroup cross-section library.

3. DRAGON ASSEMBLY MODEL

The DRAGON model directly uses the 2-group cross-sections provided by DRAGON itself after the homogenization/condensation process (Fig. 1). This second level calculation deals with

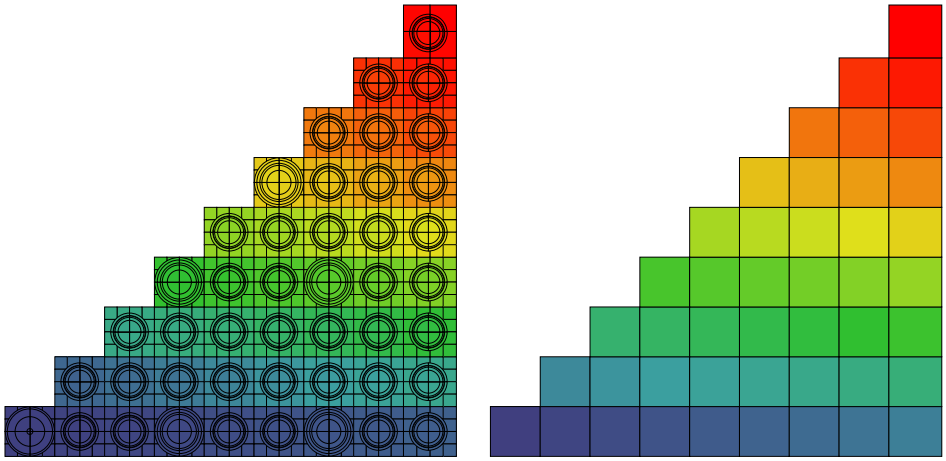

Figure 1. DRAGON assembly geometries before and after homogenization

45 homogenized cells associated with 45 different materials, each of them corresponding to an homogenized fuel pin or water hole.

3.1. Reference results

As one can see in Figure 2, each cell is subdivided in 6x6 regions to produce a 1326 region geometry (1/8th symmetry). This geometry will be considered as a reference, and its choice will be validated in the forthcoming convergence analysis.

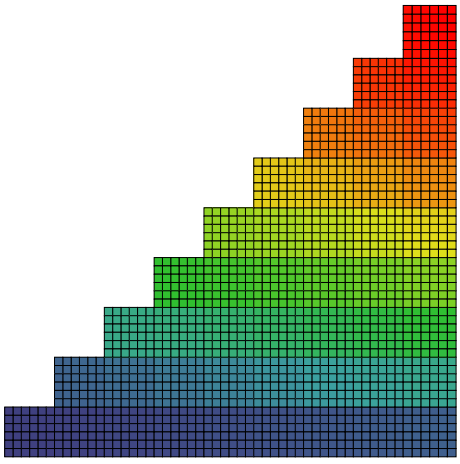

Figure 2. DRAGON assembly geometry with 6x6 discretization

The convergence criteria for the k_{eff} and the flux are respectively denoted ξ_k and ξ_ϕ. The tracking parameters $\#l$ and $\#\varphi$ represent the number of lines per cm and the number of angles used to discretize the geometry for the collision probability technique in DRAGON. The parameters selected for our reference calculation are summarized in Table I:

Table I. DRAGON calculational parameters

$\#l$	$\#\varphi$	# of groups	# of regions	# of scalar unknowns
10.0 cm^{-1}	16	2	1326	2652
k_{eff}	ξ_k	# outer	ξ_{outer}	ξ_{inner}
1.37176	10.0^{-5}	7	$5.0\ 10.0^{-5}$	$5.0\ 10.0^{-5}$

The convergence criteria that must be satisfied between iterations l and $l-1$ are: $\epsilon_k \leq \xi_k$ and $\epsilon_\phi \leq \xi_\phi$. Equation (1) defines ϵ_k and ϵ_ϕ with $\phi_i^g(l)$ the flux in the energy group g and the region i and $k_{eff}(l)$ the eigenvalue of the problem. The flux convergence criteria must be satisfied at both the inner and outer iteration level for 2 successive iterations before exiting the iteration loop.

$$\epsilon_k = \frac{\left|k_{eff}(l) - k_{eff}(l-1)\right|}{k_{eff}(l)} \quad \text{and} \quad \epsilon_\phi = \max_g \left\{ \frac{\max_i |\phi_i^g(l) - \phi_i^g(l-1)|}{\max_i |\phi_i^g(l)|} \right\} \tag{1}$$

The associated fluxes are presented Figure 3, where one can see the impact of the water holes that tend to thermalize the flux.

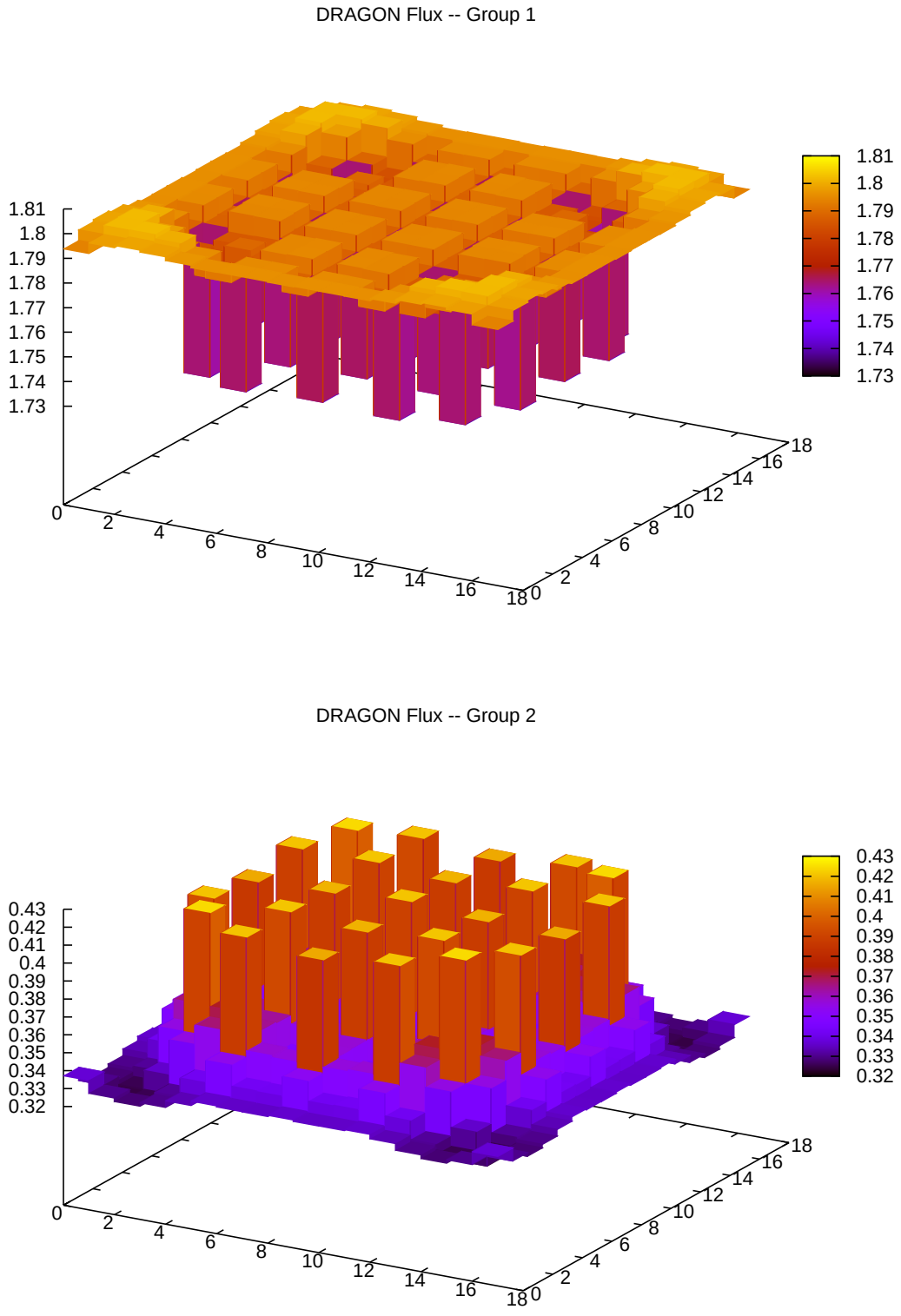

Figure 3. DRAGON fluxes

3.2. Spatial and angular convergence

In order to analyze the spatial and angular convergence, different configurations were tested by varying the spatial discretization and the tracking parameters. Table II shows that the reference configuration characterized by a 6x6 spatial discretization and 16 10.0 tracking parameters may be considered as converged.

Results are compared based on the k_{eff} and group fluxes using equation (2):

$$\delta k_{eff} = 10^5 \frac{k_{eff} - k_{eff}^{ref}}{k_{eff}^{ref}} \qquad \text{and} \qquad \min_{g,i} 100 \frac{\phi_i^g - \phi_i^{g,ref}}{\phi_i^{g,ref}} \leq \delta\phi \leq \max_{g,i} 100 \frac{\phi_i^g - \phi_i^{g,ref}}{\phi_i^{g,ref}} \tag{2}$$

Table II. DRAGON convergence analysis

Spatial	δk_{eff} (pcm)	$\delta\phi$ (%)	Tracking	δk_{eff} (pcm)	$\delta\phi$ (%)
12x12 – 16 10.0		k_{eff}=1.37173	6x6 – 64 50.0		k_{eff}= 1.37183
2x2	17	[-0.86, 0.12]	8 5.0	0	[-0.22, 0.25]
6x6	8	[-0.39, 0.05]	16 10.0	1	[-0.03, 0.02]
8x8	3	[-0.18, 0.02]	32 20.0	0	[0.00, 0.01]

The spatial relative difference is evaluated using a 12x12 fine mesh and the 16, 10.0 tracking parameters, while the angular relative difference is evaluated using a 64, 50.0 fine tracking parameter and a 6x6 spatial discretization.

4. PENTRAN ASSEMBLY MODEL

This section deals with PENTRAN calculations. PENTRAN is designed to perform parallel distributed decomposition of discrete ordinates in 3-D Cartesian geometry. One of its features is the possibility to perform a parallel decomposition of the computational effort involving space, angle, and energy group, and hybrid decomposition combinations. In this study, the assembly geometry was divided in 9 coarse meshes with a focus on purely spatial decomposition of the problem using 9 processors in parallel.

4.1. Reference results

Figure 4 shows the assembly model used with PENTRAN, each of the 289 cells are discretized using a 6x6 fine mesh (within our model, PENTRAN works on the full geometry and not the 1/8th symmetric geometry). The 3x3 coarse mesh clearly appears in the figure. This geometry will be considered as a reference, and its choice will be validated by the associated a convergence analysis.

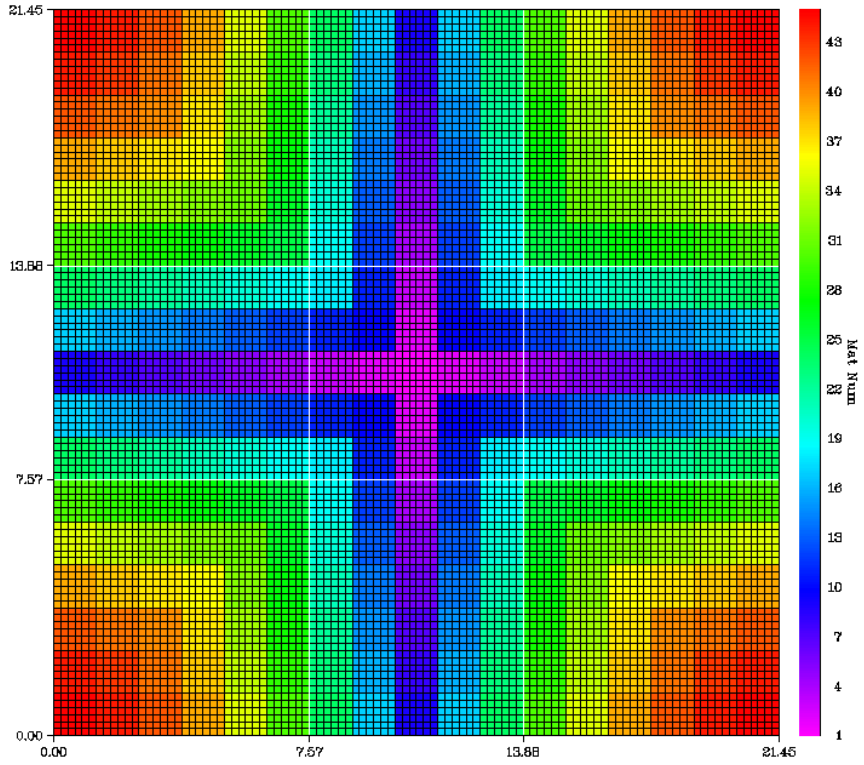

Figure 4. PENTRAN assembly geometry with 6x6 discretization

The convergence criteria for the k_{eff} and the flux were, respectively, set to 5.10^{-6} and 5.10^{-5}. The discretization of each cell is identical to that selected for DRAGON (6x6) while S_6 directions are considered for the angular quadrature. Here, we also used equation (1) to define $\epsilon_k \leq \xi_k$ and ϵ_ϕ that are supposed to verify $\epsilon_k \leq \xi_k$ and $\epsilon_\phi \leq \xi_\phi$. The calculational parameters are summarized in Table III:

Table III. PENTRAN calculational parameters

# S_n quadrature	# of groups	# of regions	# of scalar unknowns
S_6	2	10404	20808
k_{eff}	# outer	ξ_{outer}	ξ_{inner}
1.37172	36	$5.0\ 10.0^{-6}$	$5.0\ 10.0^{-5}$

4.2. Spatial and angular convergence

Comparison are made on the k_{eff} and the flux using equation (2). Table IV presents the results obtained and confirms that the reference configuration characterized by a 6x6 spatial discretization and 6 directions may be considered as converged. The spatial relative difference is evaluated using a 12x12 fine mesh and 6 directions, while the angular relative difference is evaluated using an S_{12} quadrature and a 6x6 spatial discretization. When comparing these two references, the k_{eff} appears to be converged within 50 pcm.

Table IV. PENTRAN convergence analysis

Spatial	δk_{eff} (pcm)	$\delta\phi$ (%)	Angle	δk_{eff} (pcm)	$\delta\phi$ (%)
12x12 – S_6	k_{eff}=1.37194		6x6 – S_{12}	k_{eff}= 1.37140	
2x2	-3	[-1.35, 0.58]	S_4	-17	[-0.35, 0.42]
6x6	-16	[-0.14, 0.02]	S_6	24	[-0.20, 0.21]
8x8	-28	[-0.08, 0.01]	S_8	18	[-0.09, 0.14]

When analyzing the convergence, it clearly appears that the flux difference tends to decrease while refining the mesh or increasing the quadrature. The k_{eff} behavior is less predictable, this being most probably related to numerical roundoff errors, since within each coarse mesh the contribution to k_{eff} is evaluated in single precision.

5. MCNP ASSEMBLY MODEL

The same assembly geometry was modeled with MCNP, using the same set of 2-group cross-sections. The results obtained provide a reference to be compared to DRAGON and PENTRAN results.

5.1. Calculational parameters and convergence

The number of particles simulated is equal to 1000 active cycles of 50000 particles. This resulted in a k_{eff}=1.37149 with σ=17 pcm. The typical uncertainty associated with the flux is less than to 0.2% in the thermal group and 0.1% in the fast group. Accounting for the 1/8th symmetry, the practical uncertainty shall be divided by a factor of $1/\sqrt{8}$.

5.2. Comparison with DRAGON

The k_{eff} discrepancy appears to be less than 20 pcm. In Figure 5, flux differences are less than $\pm$0.1% in the fast group ($g = 1$), while they reach $\pm$0.5% in the thermal group ($g = 2$). If no specific trend may be observed in the fast group, the greatest differences in the thermal group appear to be associated with the water holes where DRAGON underestimates the flux.

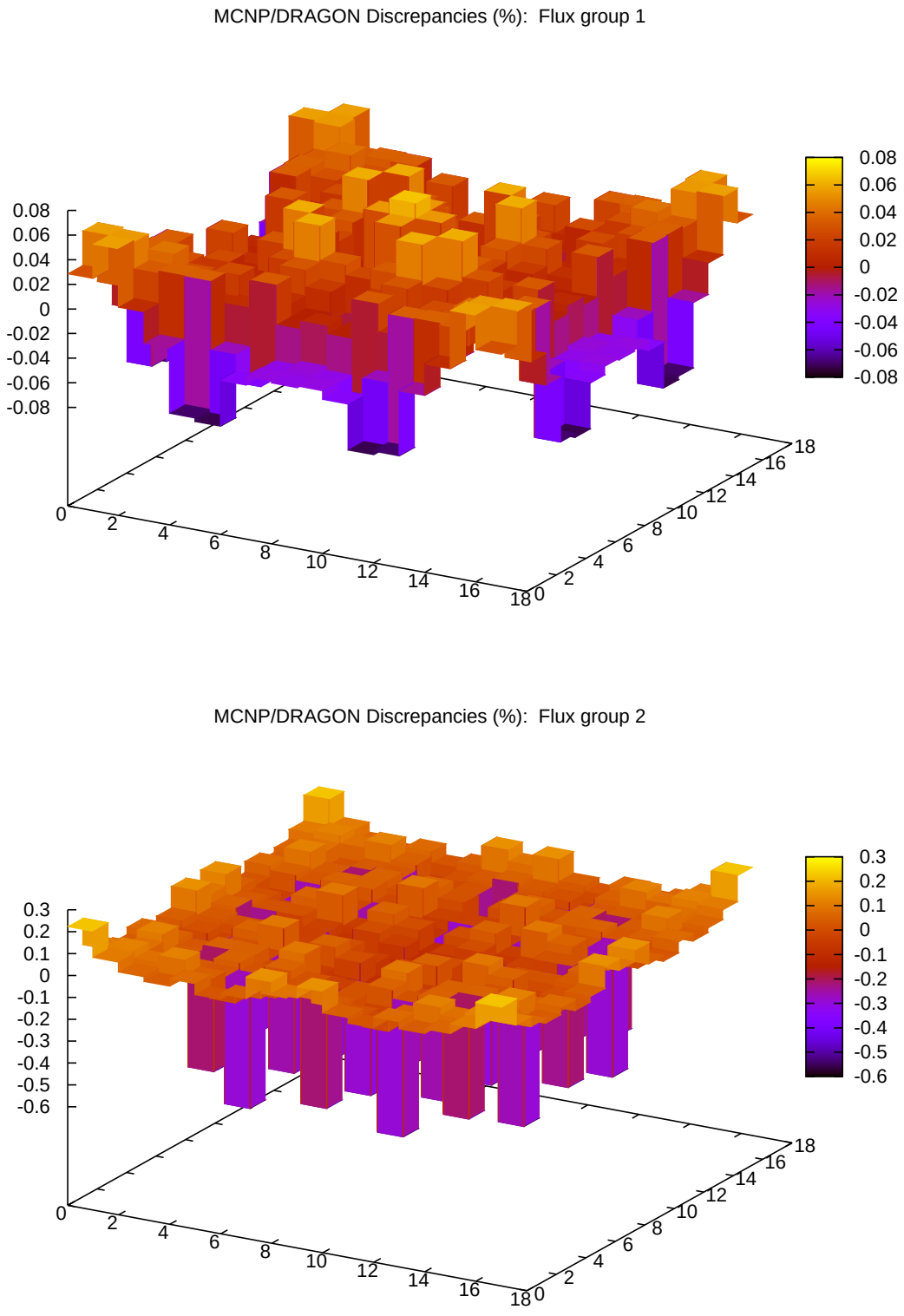

Figure 5. MCNP-DRAGON fluxes comparison

5.3. Comparison with PENTRAN

The k_{eff} discrepancy appears to be less than 20 pcm. Flux differences are within $\pm 0.5\%$ in both groups (Fig. 6). Apart from a flux underestimation in the water holes for the thermal group ($g = 2$), no specific trend may be observed in the flux differences that appear randomly distributed.

5.4. Discussion concerning the deterministic methods used

As shown previously, the two deterministic codes and methods used yield very consistent results. However, one may have an interest in highlighting their complementary features concerning this benchmark:

- The collision probability technique used in DRAGON appears to converge in much less outer iterations than the S_n method. This is most probably related to the scattering reduction operation. This consists in inverting the collision probability matrix to solve a modified set of equations where no iteration is required for the energy groups that do not involve up-scattering. Moreover, the collision probability matrix method solves a problem where the neutron flux is already integrated with respect to the angular variable. This tends to stabilize the numerical scheme compared to solving the transport equation for the angular flux and then integrating the solution.

  One may note that the collision probability technique is limited by the size of the collision probability matrix, which is proportional to the square of the number of spatial unknowns. Such a method is then well adapted to deal with assembly calculations, generally used in an industrial context to prepare homogenized and condensed cross sections for reactor core codes.

- Considering the S_n methods implemented in PENTRAN, two major features need to be discussed. Firstly, the use of S_n methods allows one to deal with high order scattering cross-sections, whereas the collision probability technique is based on transport corrected isotropic cross-sections. This feature offers the possibility to utilize more detailed nuclear data, and hopefully provides better results when comparing to experiments.

  Secondly when considering a 3D full core model, the use of the parallel capabilities of PENTRAN is of significant interest. Relying on the distributed memory parallel architecture, it is possible to deal with arbitrarily large or refined problems, provided the geometry is subdivided into a sufficient number of coarse meshes. Although only spatial decomposition was considered in the present study, PENTRAN also supports hybrid decomposition strategies involving space, energy, and angle. As a consequence of this feature, the parallel S_n method should be more efficient for 3D full core calculations.

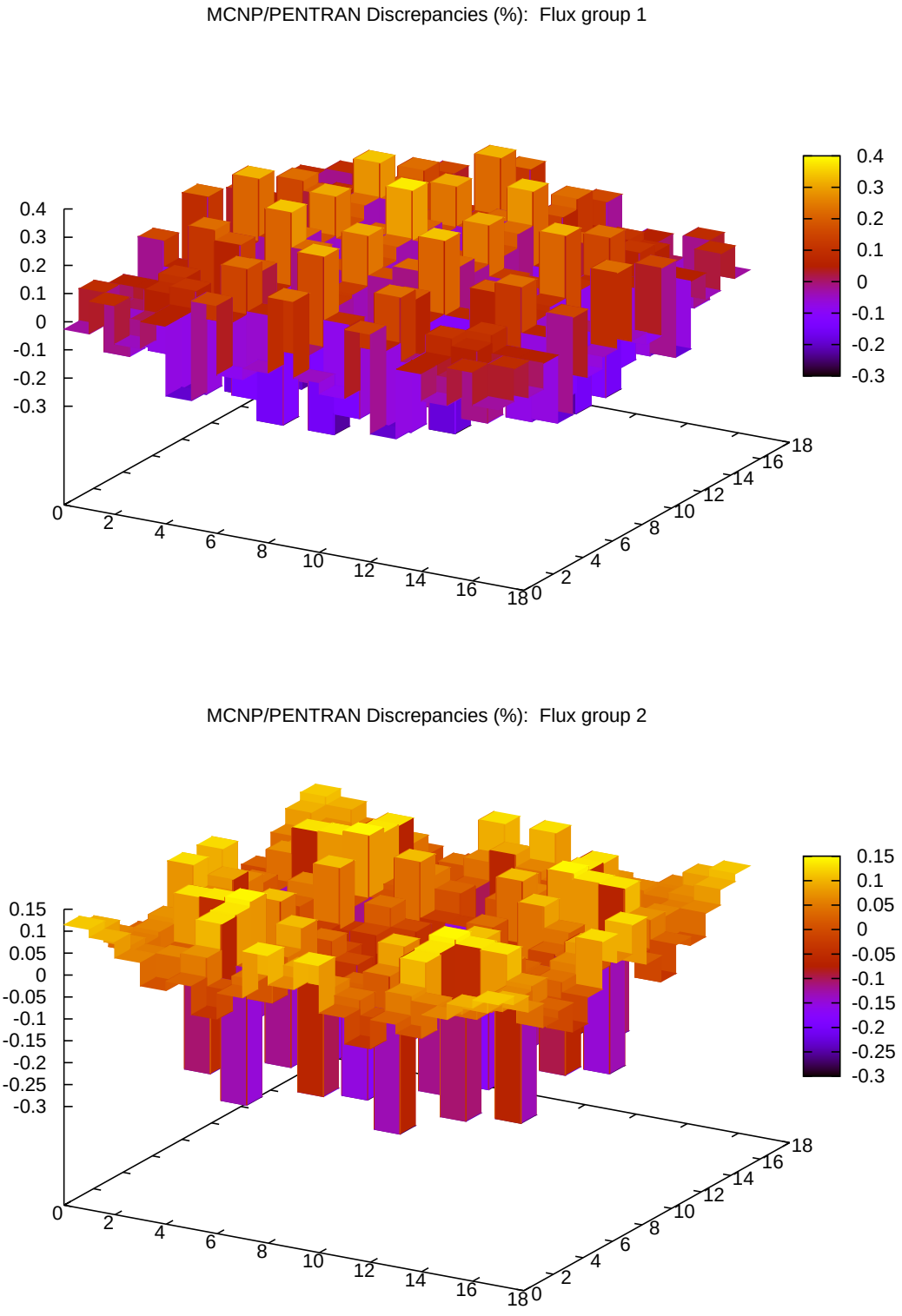

Figure 6. MCNP-PENTRAN fluxes comparison

6. CONCLUSION

The present work shows that there is a good agreement between DRAGON, PENTRAN, and MCNP when dealing with a PWR assembly described with pin-by-pin homogeneous 2-group cross-sections.

One may wish to highlight that multigroup Monte Carlo methods offer an interesting approach to perform systematic validation of deterministic solvers, provided one can produce multigroup cross-section libraries in a format compatible with MCNP.

This paper shows that DRAGON and PENTRAN yield consistent results when relying on similar discretization parameters: 6x6 spatial discretization, and 16 tracking directions with DRAGON or S_6 angular quadrature with PENTRAN. Comparison with MCNP shows that the k_{eff} difference is less than 20 pcm and that the flux discrepancies are within $\pm 0.5\%$ for PENTRAN and DRAGON.

Based on these results, further work will address a full 3D core PWR benchmark comparing PENTRAN and MCNP. Such a benchmark is anticipated to be challenging with respect to the size of the problem. The use of comprehensive parallel computers appears to be a promising approach enabling one to compute reference fluxes and reaction rates with a deterministic neutron transport S_n solver.

However and even if a transport–transport equivalence is used, a two-group transport approach may not yield satisfying results with respect to energy, especially if strong spectrum transients are considered such as UOX/MOX and/or fuel/reflector interfaces. Prior to dealing with full core problems, an analysis must be performed to determine the adequate energy discretization. Based on the analyses devoted to reference transport calculations for PWR reactors [9], the number of energy groups required to capture the spectrum effects is typically less than 50, provided the discretization is optimized.

7. ACKNOWLEDGEMENTS

The authors want to thank Joël Le Mer from EDF R&D for providing useful information regarding cross-section generation with DRAGON.

REFERENCES

[1] G. MARLEAU, A. HÉBERT, and R. ROY, "A User Guide for DRAGON 3.05", Report IGE-174 Rev. 6, 2006, Institut de Génie Nucléaire, École Polytechnique de Montréal, Québec, Canada.

[2] G. E. SJODEN and A. HAGHIGHAT, "PENTRAN, a Parallel Environment Neutral Particle TRANsport Code in 3-D Cartesian Geometry", *Mathematics Methods and Supercomputing for Nuclear Applications*, Saratoga Springs, NY 1997.

[3] G. E. SJODEN and A. HAGHIGHAT, "PENTRAN, a Parallel Environment Neutral Particle TRANsport Code in 3-D Cartesian Geometry", *Code Users's Guide/Manual, Version 9.4.X.5*, HSW Technologies LLC, November 2008.

[4] X-5 Monte Carlo Team, "MCNP - A General Monte Carlo N-Particle Transport Code. Version 5, Volume I: Overview and Theory." Report LA-UR-03-1987, April 2003 (Revised March 2005).

[5] "IAEA-Nuclear Data Services, WIMS Library Update Project", http://www-nds.iaea.org/wimsd/libraries.htm

[6] J. LE MER, G. MARLEAU, and T. COURAU, "Elements of Validation of the Code DRAGON vs MCNP5 for PWR assembly calculations", *International Conference on the Physics of Reactors*, Interlaken Switzerland, September 2008.

[7] A. HÉBERT, "A Consistent Technique for the Pin-by-Pin Homogenization of a Pressurized Water Reactor Assembly", *Nuclear Science and Engineering*, **113**, 227–238 (1993).

[8] "Python Programming Language", http://www.python.org

[9] J. VIDAL, O. LITAIZE, D. BERNARD, A. SANTAMARINA, C. VAGLIO-GAUDARD, and R. TRAN, "A New Modeling of LWR Assemblies using the APOLLO2 Code Package", *Mathematics & Computation and Supercomputing Nuclear Applications, M&C+SNA 2007*, Monterey, CA, USA (2007).